Chinese Chemical Letters 37 (2026) 111910

Contents lists available at ScienceDirect

Chinese Chemical Letters

journal homepage: www.elsevier.com/locate/cclet

The applied progress and prospects of sub-nanometer high-entropy materials in the fields of electrocatalysis and biomedicine: Review and outlook

Zhiyu Shao[b,1], Shaohua Wang[a,1], Haijia Yu[c], Diyang Shan[a], Zhiyu Tang[a], Yihang Fu[d], Jianshi Du[b,*], Jianhua Liu[c,*], Keke Huang[a,*]

[a] State Key Laboratory of Inorganic Synthesis and Preparative Chemistry, Jilin Provincial International Cooperation Key Laboratory of Advanced Inorganic Solid Functional Materials, College of Chemistry, Jilin University, Changchun 130012, China
[b] China-Japan Union Hospital of Jilin University, Changchun 130061, China
[c] Department of Radiology, the Second Hospital of Jilin University, Changchun 130041, China
[d] Yale University, New Haven, CT 06511, United States

ARTICLE INFO

Article history:
Received 3 August 2025
Revised 18 September 2025
Accepted 27 September 2025
Available online 29 September 2025

Keywords:
High entropy materials
Sub-nanometer
Electrocatalyst
Biomedical materials
Nanostructure

ABSTRACT

Sub-nanometer high-entropy materials (HEMs) have opened new pathways in electrocatalysis and biomedicine, leveraging their tunable composition, ultrahigh specific surface area, abundant active sites, and multi-element synergy. In electrocatalysis, their highly disordered multi-element structures significantly enhance the intrinsic activity and stability for the hydrogen evolution reaction (HER), oxygen evolution reaction (OER), and CO_2 reduction reaction (CO_2RR), while their unique "cocktail effect" enables precise electronic structure modulation. For biomedical applications, their ultrasmall size facilitates cellular uptake and tissue penetration. Simultaneously, their multi-element composition endows them with multifunctionality, including photothermal/photodynamic/catalytic/magnetic therapy, multimodal imaging, and drug delivery, while also optimizing biocompatibility and reducing toxicity. However, challenges remain in the precise synthesis and mechanistic understanding of sub-nanometer HEMs, hindering their development for next-generation high-performance electrocatalysts and intelligent theranostic platforms. In this review, we comprehensively explore the composition-structure design principles of HEMs, with a focus on the multifunctional properties achieved by small sizes, particularly in the sub-nano range, and their applications in electrocatalysis and biomedicine. Additionally, this paper prospectively discusses emerging strategies that may drive the future development of HEMs, with particular emphasis on the application potential of sub-nanometer HEMs.

© 2026 Published by Elsevier B.V. on behalf of Chinese Chemical Society and Institute of Materia Medica, Chinese Academy of Medical Sciences.

1. Introduction

High-entropy materials (HEMs) refer to materials that contain five or more elements in nearly equal proportions within the same crystal structure [1,2]. Unlike traditional materials, which are typically composed of one or a few elements, the uniqueness of HEMs lies in their complex composition and high entropy characteristics [3–5]. The core of this concept is the increase in entropy, meaning that by introducing multiple elements [6,7], the disorder of the material is significantly enhanced [8], thereby improving its performance and stability [9]. However, conventional materials face limitations due to elemental constraints [10–13], reaching a performance bottleneck. In response, Cantor *et al.* independently introduced the concept of HEMs in 2004, homogeneous multi-component alloys with near-equimolar atomic ratios [14]. Thermodynamically, these alloys exhibit high mixing entropy, which overcomes enthalpy-driven limitations [15–17]. Since their discovery, HEMs have sparked extensive research interest in both scientific and industrial communities [18,19], with applications spanning catalytic energy conversion, energy storage technologies, and biomedical materials [20–22]. Their continuously tunable compositional distributions break the miscibility barriers of traditional materials [23,24], providing ideal adsorption/desorption energetics for reaction intermediates [25,26]. Furthermore, advances in nanotechnology have enabled significant improvements

* Corresponding authors.
E-mail addresses: dujs@jlu.edu.cn (J. Du), jian_hua@jlu.edu.cn (J. Liu), kkhuang@jlu.edu.cn (K. Huang).
[1] These authors contributed equally to this work.

https://doi.org/10.1016/j.cclet.2025.111910
1001-8417/© 2026 Published by Elsevier B.V. on behalf of Chinese Chemical Society and Institute of Materia Medica, Chinese Academy of Medical Sciences.

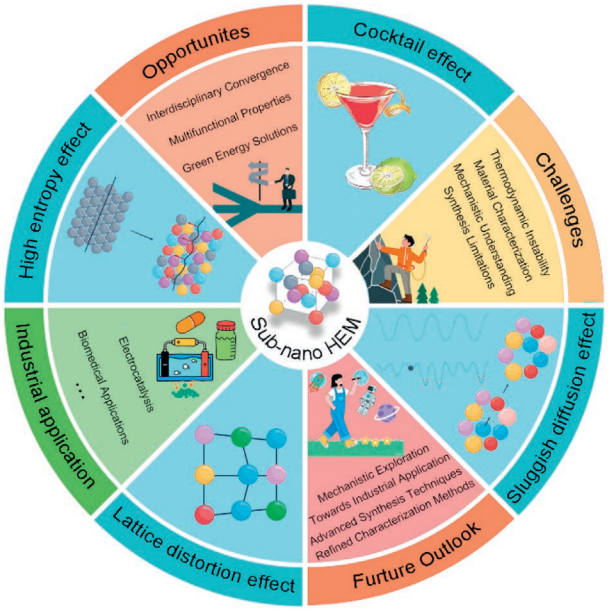


Fig. 1. The major effect mechanisms, opportunities, challenges, and outlook of HEMs.

in surface activity through geometric engineering and electronic state modulation [27,28]. The integration of nanomaterial concepts have led to the development of nano and even sub-nano HEMs, which have garnered widespread attention in fields such as energy conversion and catalysis due to their enhanced functionality [29,30].

The introduction of the sub-nanoscale (typically referring to feature sizes below 1 nanometer) has opened up an entirely new dimension for HEMs [31–33]. At this critical scale, materials exhibit remarkable quantum confinement effects, extremely high specific surface areas, unique electronic structures, and highly exposed and tunable active sites. When the structural units of HEMs are precisely reduced to the sub-nanoscale. A "quintuple synergy" unprecedented synergy emerges: the compositional flexibility and unique electronic structure conferred by "high entropy" synergize powerfully with the ultimate atomic utilization efficiency and ultra-strong surface/interface effects bestowed by the sub-nanoscale [34–36]. This synergistic effect not only effectively overcomes the inherent limitations of conventional HEMs in catalysis and biological applications but also drives remarkable performance leaps in cutting-edge fields such as electrochemical energy conversion, biosensing, and diagnostic-therapeutic integration. We systematically summarize rational design strategies for Sub-nano HEMs structures, including: (1) Non-equilibrium thermodynamic synthesis [37], (2) control of (sub)nanometer dimensions and anisotropic morphologies [38], and (3) engineering of atomic ordering/disordering [39]. Specifically, size regulation and multidimensional architectures are recognized as two crucial trends in developing HEMs.

Although recent reviews have reported on the advantages and synthesis of HEMs [40–43], there is still a lack of reviews specifically focusing on recent progress, emerging roles, or fundamental design principles for sub-nanometer HEMs in catalysis and emerging fields of biomedicine. Herein, we provide a systematic review of advances in sub-nanometer HEMs, focusing on structure-property relationships, catalyst-support interactions, and potential applications. Finally, we outline key challenges and future research directions to guide researchers in this emerging field (Fig. 1).

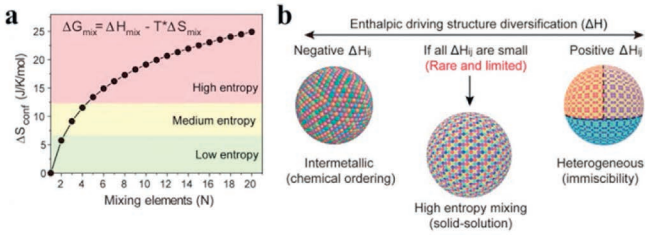


Fig. 2. Thermodynamic analysis of high-entropy mixing considers both entropy (a) and enthalpy (b), which are mainly determined by the composition of high-entropy nanoparticles. Reproduced with permission [46]. Copyright 2022, AAAS.

2. Synthesis of sub-nanometer HEMs

The key challenge in fabricating HEMs lies in suppressing phase separation [44,45]. The configurational entropy of high-entropy nanoparticles increases with a greater number of elements and acts as a driving force for single-phase mixing (Fig. 2a). The enthalpy of the multielement interactions varies largely depending on the nature of the constituent elements, which directly affects the resulting phase under near-equilibrium conditions (Fig. 2b) [46]. Traditional thermodynamics-driven synthesis methods, such as metallurgy, electrospinning, and wet chemistry, rely entirely on the Gibbs free energy of the material system to determine phase stability, expressed as:

$$\Delta G_{\mathrm{mix}} = \Delta H_{\mathrm{mix}} - T\Delta S_{\mathrm{mix}}\Delta H_{\mathrm{mix}} \quad (1)$$

where ΔG_{mix}, ΔH_{mix}, ΔS_{mix} and T denote the Gibbs free energy, mixing enthalpy, mixing entropy, and absolute temperature, respectively.

As entropy-dominated materials, high-entropy systems must account for various entropy contributions, including configurational, vibrational, electronic, and magnetic dipole entropy. Among these, configurational entropy plays the dominant role. Under ideal conditions, it can be calculated as:

$$\Delta S_{\mathrm{conf}} = -R\sum x_i ln x_i \quad (2)$$

where R is the gas constant, and x_i represents the molar fraction of the element.

Recently, kinetics-driven synthesis has emerged as a crucial strategy for HEMs' formation. By leveraging rapid non-equilibrium processes, metastable high-entropy phases can be kinetically trapped through localized extreme conditions, ensuring phase homogeneity. For instance, ultrafast heating and cooling can anchor single-phase solid solutions in energy minima, effectively preventing phase separation.

When high-entropy materials achieve sub-nanometer structures, their high surface atom exposure ratio and electron delocalization effects enhance their catalytic performance in heterogeneous catalysis. In sufficiently small volumes, surface energy becomes non-negligible, leading to the expression $G_{\mathrm{total}} = G_{\mathrm{bulk}} + G_{\mathrm{surface}}$, where $G_{\mathrm{surface}} = \gamma_{(\mathrm{T})}A_{(\mathrm{T})}$ plays a decisive role. Consequently, overcoming surface energy to achieve controllable synthesis and precise morphological regulation remains a near-term priority in the development of high-entropy materials. Although numerous high-entropy nanomaterials have been synthesized, reliably controlling their size to ≈1 nm remains a significant challenge due to high surface energy. Current high-entropy nanomaterials primarily suffer from elemental immiscibility due to compositional differences and complexity. Therefore, non-equilibrium synthesis techniques involving extreme temperatures, pressures, or external energy fields remain essential for achieving uniform elemental mixing and reducing particle size [47].

Beyond conventional high-entropy synthesis, achieving sub-nanometer-scale materials demands even more stringent conditions. Sub-nanometer HEMs formed *via* homogeneous nucleation exhibit significant biomedical advantages due to their enhanced metabolic clearance, thereby minimizing potential toxicity. However, calculating ΔG for such materials require additional consideration of interfacial tension (σ) and surface area (A):

$$\Delta G = -n\Delta\mu + \sigma A \quad (3)$$

where $\Delta\mu$ is the chemical potential difference.

In contrast, heterogeneous nucleation introduces a correction term:

$$\Delta G = \varphi\Delta G^{*} \quad (4)$$

Here, φ is the contact angle function:

$$\varphi = \left(2 + cos\theta\right)\left(1 - \cos\theta\right)^{2}/4 \quad (5)$$

Notably, only when $\theta = \pi$ does the nucleation rate of heterogeneous nucleation match that of homogeneous nucleation. For all other contact angles, the energy barrier for heterogeneous nucleation is lower, making it the more favorable pathway. Thus, selecting suitable substrates to mediate interfacial tension offers a viable route for synthesizing sub-nanometer high-entropy materials.

3. Core mechanism of HEMs

The unique properties of HEMs primarily stem from four distinct effects that differentiate them from conventional materials: (1) High-entropy effect: Stabilizes single-phase solid solutions by maximizing configurational entropy; (2) Lattice distortion effect: Results from atomic size mismatch, leading to localized strain and modified electronic structures. (3) Sluggish diffusion effect: Slows atomic migration due to compositional complexity, enhancing thermal and kinetic stability. (4) Cocktail effect: Synergistic interactions among multiple elements yield emergent properties beyond linear combinations. These effects collectively explain the unusual phenomena observed in HEMs and have been experimentally validated over the years of research. Notably, as the size decreases, these effects become more pronounced. In this section, we discuss the fundamental mechanisms of these four core effects, providing insights for the rational design of novel HEMs.

3.1. High-entropy effect

The high-entropy effect is a defining characteristic of HEMs, which inhibits the formation of brittle, stoichiometric compounds with strongly ordered atomic arrangements. Instead, this effect promotes the stabilization of solid solutions. Due to the dominant role of entropy, equimolar multi-component alloys (even those with up to 20 elements) preferentially adopt face-centered cubic (FCC) crystal structures in most cases.

3.2. Lattice distortion effect

The concept of lattice distortion has a long history in physical metallurgy. Typically, HEMs contain solid-solution phases with multiple principal elements, where all atoms in the system act as solute atoms. This results in neighboring atoms with different atomic radii and asymmetric bonding, inevitably causing deviations from their average lattice positions.

Lattice distortion influences various material properties and reduces thermal effects. Many studies have reported the contribution of severe lattice distortion to the mechanical properties of HEMs. It has also been shown that distorted atomic planes in some HEMs enhance X-ray diffuse scattering, leading to weaker peak intensities. This distortion also increases electron scattering, significantly reducing electrical conductivity. Additionally, severe lattice distortion enhances phonon scattering, further lowering thermal conductivity.

3.3. Sluggish diffusion effect

The sluggish diffusion effect is inherently derived from the lattice distortion effect characteristic of HEMs. It is well known that atomic diffusion occurs more rapidly in amorphous regions or along grain boundaries. Additionally, body-centered cubic (BCC) structures exhibit faster diffusion rates than FCC structures due to their lower atomic packing density. However, compared to conventional materials with uniform bond lengths and strengths, HEMs with severe lattice distortion possess aperiodic atomic traps. This contrasts sharply with the regular energy fluctuations in perfect crystalline lattices of pure elements. While atoms at low-energy sites have a higher probability of escaping their positions, those trapped in short-range atomic wells face significantly higher energy barriers and activation energies for diffusion. This effectively suppresses sustained atomic diffusion behavior. The resulting sluggish diffusion contributes to the exceptional thermal stability and kinetic resistance to phase separation observed in HEMs, even at elevated temperatures. This phenomenon has been experimentally verified through tracer diffusion studies and molecular dynamics simulations in various HEM systems.

3.4. Cocktail effects

The cocktail effect in HEMs highlights performance enhancement through synergistic interactions among multiple elements, suggesting that atomic-scale composite behavior can yield unexpected functionalities. Incorporating specific elements can modulate material properties including density, oxidation resistance, wear resistance, and electrical conductivity. However, the current understanding of this cocktail effect remains incomplete, necessitating further research to elucidate its fundamental mechanisms.

Sub-nanometer materials typically exhibit significant sub-nanometer-scale phenomena, such as pronounced quantum confinement effects. As the size of nanoparticles decreases, the proportion of surface atoms increases dramatically. However, when the size reaches the sub-nanometer level, strong surface energy arises between the nanoparticles. As a result, nanoparticles tend to aggregate to balance this high surface energy. Therefore, developing synthesis methods for sub-nanometer ultra-small HEMs remains a common goal among researchers.

4. Synthesis method of sub-nanometer HEMs

The synthesis of HEMs typically relies on the mixing of multiple metal salt precursors to achieve a solid solution with maximum mixing entropy. Traditionally, HEAs have been synthesized mainly through melting or plasma methods, which can produce atomic mixed phases. However, the preparation of nanostructured alloys often employs wet chemical synthesis, which involves co-reduction of metal salts with capping agents to prevent crystal growth and aggregation. Due to differences in the reaction rates of various metal salts, this method is limited in the types of alloys that can be synthesized. Furthermore, scaling down high-entropy alloys to the nanoscale is a highly challenging task [48].

To date, numerous synthesis strategies for HEMs have been developed, which can be generally categorized into three main approaches: Solid-phase, liquid-phase, and gas-phase processing. Solid-phase methods involve grinding metal salts or metals, thermal decomposition, and other processing techniques to directly form nano powders from their respective solid phases [49,50]. Liquid-phase processing, including arc melting, induction melting,

and metal spray techniques, has been used to prepare HEMs. Gas-phase processing of high-entropy alloys involves converting metal salt precursors into gaseous states and then solidifying the desired materials under specific atmospheres [51]. Despite the many traditional and modern methods for preparing HEMs, exploring new synthesis methods for HEMs with ideal properties has become one of the most important research topics in this field.

5. Size-miniaturization of HEMs

For bulk materials, non-surface atoms cannot directly interact with reaction intermediates in catalytic systems, which fundamentally limits the catalyst's performance ceiling. However, reducing the material size to nanoscale or even sub-nanoscale/cluster dimensions can maximize the utilization of surface-active atoms. Notably, as material dimensions decrease, the number of exposed surface atoms increases exponentially, creating vast possibilities for the development of catalysts. This has driven significant research interest in sub-nanometer materials. Sub-nanometer materials exhibit unique characteristics including discrete electronic energy levels, pronounced surface/interface effects, and quantum size/macroscopic quantum effects - collectively termed as the "nano-size effect". Sub-nanometer HEMs inherit these properties while achieving a synergistic "nano-high-entropy" effect. However, traditional materials at extremely small sizes demonstrate strong surface energy. To minimize this energy, adjacent nanoparticles tend to aggregate, particularly when particle size falls below 2 nm, leading to substantial degradation of material functionality. To address this challenge, researchers have developed various strategies to prevent nanoparticle agglomeration, including confinement engineering, self-assembly methods, and template approaches, all aimed at optimizing both functionality and stability of these advanced materials.

For traditional bulk materials, the limited number of surface atoms restricts their catalytic activity. Reducing the material size to the nanoscale can significantly increase the ratio of surface atoms to total atoms, thereby improving atomic utilization efficiency. This approach holds the potential to enhance material performance beyond that of single-element nanoparticles [52]. At the nanoscale, high-entropy materials exhibit unique phenomena not observed in their bulk counterparts, including size-dependent effects, enhanced surface and interfacial effects, quantized electronic energy levels, as well as quantum size and macroscopic quantum tunneling effects [53]. The regulation of nanomaterial surface chemical activity by size plays two key roles: First, it weakens the binding strength between the solid energy bands and surface valence orbitals, enhancing the tendency and intensity of surface atoms to form surface coordination bonds; Second, it amplifies the influence of other structural factors by attenuating energy band strength. For instance, the specific surface area (surface area-to-volume ratio) of spherical particles is inversely proportional to their diameter. When the particle size decreases from 10 nm to 1 nm, the proportion of surface atoms increases from 50 % to 99 %, with nearly all atoms existing in a surface state.

This vast surface area significantly elevates the surface free energy, residual valence, and bond strength of nanoparticles, resulting in non-equilibrium and non-integer coordination of surface chemical valence [54]. Moreover, the electronic properties exhibit pronounced size-dependent behavior. The overall electronic characteristics of a material are influenced by the overlap of atomic orbitals across all atoms. In supported catalysts, electron transfer may occur between the active material and the substrate due to differences in their Fermi levels. Larger interfacial areas and higher surface-to-volume ratios lead to more significant changes in the junction effects and catalytic performance of the material [55]. Additionally, other factors such as geometric effects, dimensional effects [56], and spatial confinement effects [57] also significantly influence the material's physical properties (*e.g.*, viscosity, density) and chemical properties (*e.g.*, catalytic behavior, photosensitivity). Therefore, the synthesis of high-entropy nanomaterials with controlled size, morphology, structure, and reaction performance has remained a key research focus in the field of HEMs. Owing to their high specific surface area, unique coordination environments, unconventional local configurations, electron delocalization, and distinctive spatial arrangements, high-entropy sub-nanometer materials often exhibit unprecedented catalytic active sites.

5.1. Applications of sub-nanometer HEMs in electrochemistry

Due to several key advantages of HEMs as described in Section "2. Advantages of HEMs", these materials have seen rapid development in electrocatalysis. Essentially, they regulate adsorption energy through the hybridization of electrons at asymmetric sites. Therefore, it is possible to optimize ligands, components, or crystal phases to achieve synergistic effects between sites, thereby further dominating the electrocatalytic activity and stability of HEMs. At present, various HEMs have been applied to the field of electrocatalysis through rational regulation of electronic states, such as in promising reactions like water electrolysis electrocatalysis, fuel cells, and small molecule oxidation. To emphasize the importance of HEMs as electrocatalysts in catalysis, this section selects several key electrocatalytic reactions as representatives to introduce the significant progress of HEMs in the field of electrocatalysis.

Advances in material innovation and a deeper understanding of reaction mechanisms will be key to addressing the challenges of high overpotentials and slow kinetics in electrocatalysis. HEMs, with their multi-component and homogeneous distribution, are candidates for multi-level electronic synergy. The abundant electronic interactions in HEMs are key to achieving deep oxidation, which is essential for activating the lattice oxygen mechanism (LOM). HEMs increase configurational entropy by incorporating multiple elements (*i.e.*, chemical disorder). This redistributes electronic energy levels, potentially enhancing electron transfer and catalytic activity. Chemical disorder allows for variable surface adsorption energies, enabling flexible adsorption and desorption and optimizing reaction pathways. Their dynamic characteristics also provide self-healing abilities, adapting to environmental changes and maintaining stable catalytic performance. However, there is still a lack of guidelines for designing and constructing thermodynamically favorable LOM pathways in a targeted manner. Although HEMs have attracted widespread attention for their potential in the oxygen evolution reaction (OER) and several materials have been reported, identifying effective synergistic reaction sites remains an unresolved challenge. For example, the specific role of each constituent element in catalytic activity remains unclear, and sub-nanometer high-entropy catalysts with higher atomic utilization are still to be developed.

5.1.1. Sub-nanometer HEMs in water splitting

To obtain clean energy, water splitting for hydrogen production has been identified as one of the efficient and environmentally friendly technologies available under ambient conditions. Regulating the adsorption/desorption energies of adsorbed hydrogen (H*) for the hydrogen evolution reaction (HER) and oxygen-containing intermediates (O*, HO* and HOO*) for the OER can generate the most outstanding catalytic activity. Notably, the diversity in composition and structure, as well as the unique advantages such as the high-entropy effect of HEMs allows for continuous regulation of the electronic structure of the catalyst surface, which is conducive to breaking the scaling relationships in traditional electrocatalysis. As a result, excellent catalytic performance can be achieved in both acidic and alkaline electrolytes. Zhang *et al.* [58]

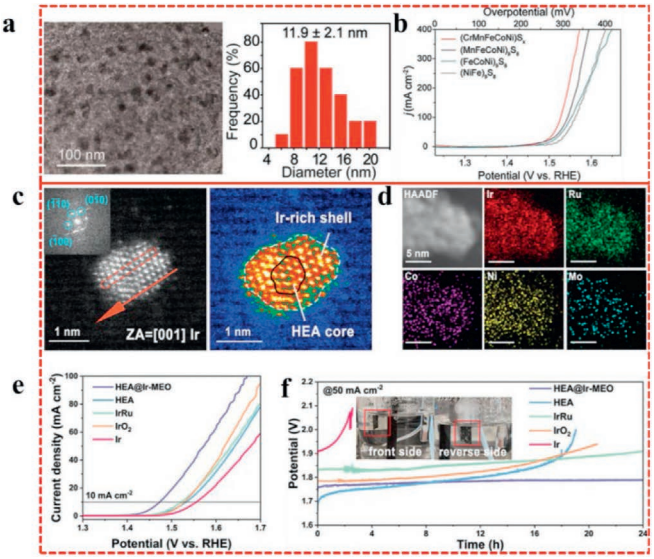


Fig. 3. (a) TEM image of the HES nanoparticles and particle size analysis. (b) LSV curves of HES. Reproduced with permission [59]. Copyright 2021, Wiley-VCH. (c) HRTEM image of HEA@Ir-MEO. Inset is the particle size analysis of the HEA@Ir-MEO. (d) HAADF-STEM image and elemental mappings of the HEA@Ir-MEO. (e) LSV curves of HEA@Ir-MEO. (f) Chronopotentiometry test curves of HEA@Ir-MEO. Reproduced with permission [62]. Copyright 2024, Wiley-VCH.

synthesized $NiFeCoCrW_{0.2}$ high-entropy alloy (HEAs), which effectively activated the LOM through synergistic multi-path electron transfer, achieving an overpotential of 220 mV at a current density of 10 mA/cm^2. It also exhibited good stability, with the potential remaining unchanged by less than 5 % of the current density at 100 mA/cm^2 over 90 days. Besides, Cui *et al.* [59] first synthesized CrMnFeCoNi sulfide (HES) solid solution nanoparticles *via* a pulsed thermal decomposition method, and particle size has reached 12 nm (Fig. 3a). Computational and X-ray photoelectron spectroscopy analyses indicated that the metal atoms exhibited synergistic effects, resulting in unique electronic states to enhance OER activity (a low overpotential of 295 mV at 100 mA/cm^2, Fig. 3b) and good durability. Subsequently, to obtain catalysts with high atomic utilization, Cai *et al.* [60] designed highly exposed ultrasmall (~5.2 nm) high-entropy sulfides confined in porous carbon nanofibers. This structure involved a synergistic effect of dual engineering of d-p orbital hybridization and nano-confinement. Calculations revealed the hybridization between the transition metal 3d orbitals and the sulfur 3p orbitals. This orbital interaction induced the movement of the d-band center towards the Fermi level, promoting the redistribution of interfacial charges and endowing HES with superior electron-donating ability to accelerate proton-coupled electron transfer kinetics. This electronic modulation significantly optimized the adsorption of OER intermediates (*OH, *O, *OOH). Experiments showed that HES had excellent OER performance, with an overpotential as low as 200 mV at 10 mA/cm^2 and negligible current attenuation after operating for 300 h at current densities ranging from 10 mA/cm^2 to 100 mA/cm^2. The dual optimization strategy of advanced electrocatalyst design through orbital hybridization engineering and size engineering has provided a new pathway for the design of energy conversion technologies. High-entropy transition metal phosphates (HEPi) have also been successfully synthesized. Qiao *et al.* [61] first reported the synthesis of HEPi catalysts (*i.e.*, CoFeNiMnMoPi) in the form of highly uniform spherical particles *via* a high-temperature flyover method. This method enabled uniform confinement of metal and phosphorus precursors in an aerosol droplet, *in situ* oxidation of oxides to phosphates at high temperatures, and uniform mixing of multimetal elements in the phosphate structure within a few milliseconds. For further tuning of morphology and size, Yao *et al.* [62] reported the synthesis of $IrRuCoNiMo@IrRuNiMoO_x$ nanoparticles (HEA@Ir-MEO) *via* a rapid liquid reduction combined with surface current displacement strategy (Figs. 3c–f). By constructing an alloy/oxide form, the Ir-rich MEO shell was conducive to maintaining structural stability and protecting the internal metals from severe dissolution during the OER process, thereby exhibiting structural stability. Its excellent electrocatalytic activity also changed the OER catalytic mechanism through the construction of high-entropy alloys.

5.1.2. Sub-nanometer HEMs in fuel cells

Fuel cells, due to their low operating temperature and high power density, have been widely used in various fields, including vehicles and portable electronics. Among them, Li-O and Zn-O fuel cells have been proven to be applicable in vehicles and portable electronic devices. The oxygen reduction reaction (ORR) is a key cathodic half-reaction in fuel cells, but its slow kinetics severely hinder the development of fuel cells. A widely accepted rule for designing efficient ORR catalysts is that the electronic structure of the catalyst surface should have the optimal adsorption/desorption strength for oxygen-containing intermediates. Although this theory fits monometallic or traditional bimetallic alloys, the complexity of the surface of HEMs, including factors such as the d-band center and coordination number, makes it necessary to develop new descriptors based on high-entropy structures to predict the adsorption/desorption energies of *OH and *O on the surface of HEMs, thereby constructing corresponding linear regression models. Xia *et al.* [63] demonstrated the excellent ORR electrocatalytic performance of structurally ordered PtIrFeCoCu high-entropy alloy (PIFCC–HEI) nanoparticles (Figs. 4a–c). At 0.85 V, it achieved an ultra-high mass activity of 7.14 A/mg of precious metals, with extraordinary durability exceeding 60,000 potential cycles. Moreover, a fuel cell assembled with PIFCC–HEI/C as the cathode provided a peak power density of 1.73 W/cm^2 at 1.0 bar backpressure (Fig. 4d), with almost no working voltage decay after 80 h of operation (Figs. 4e and f), proving its outstanding performance.

Wang *et al.* [64] incorporated phosphomolybdic acid into the synthesis of BiCuFeCeWPtOx-PMA nanowires (SNWs) high-entropy oxides (HEO) as cathode catalysts in Li-O_2 batteries (LOBs). By employing a "cluster-core co-assembly" strategy, they formed well-defined polyoxometalate (POM) clusters with a size of ~1 nm (Figs. 4g and h). The special sub-1 nm structure enabled nearly 100 % atomic exposure, meaning that most metal oxides only needed to be bonded to the material surface. As the variety of metal oxides increased, the surface and configurational entropy were enhanced, significantly reducing the activation energy for HEO formation. This was the primary reason HEOs could be formed at lower temperatures compared to traditional high-temperature methods (>1000 °C). As shown in Fig. 4i, the impact of elemental intrinsic activity on battery performance has been investigated. BCFCWPOx-PMA SNW-based LOBs demonstrated the specific capacity of 11,206 mAh/g and long-term stability of 213 cycles. The entropy modulation effect also has the impact on specific capacity, which brought the discharge capacity to gradually increase (Figs. 4j and k). Developing HEMs with various morphologies has significant application value.

5.1.3. Sub-nanometer HEMs in electrocatalytic small molecule oxidation

The electrochemical oxidation of small molecules holds great promise for replacing OER or hydrogen oxidation reaction (HOR) to enhance reaction kinetics and reduce energy consumption, as well as for producing high-value chemicals or serving as fuels [65]. Zhan *et al.* synthesized a kind of PtRuNiCoFeMo HEA SNWs for the

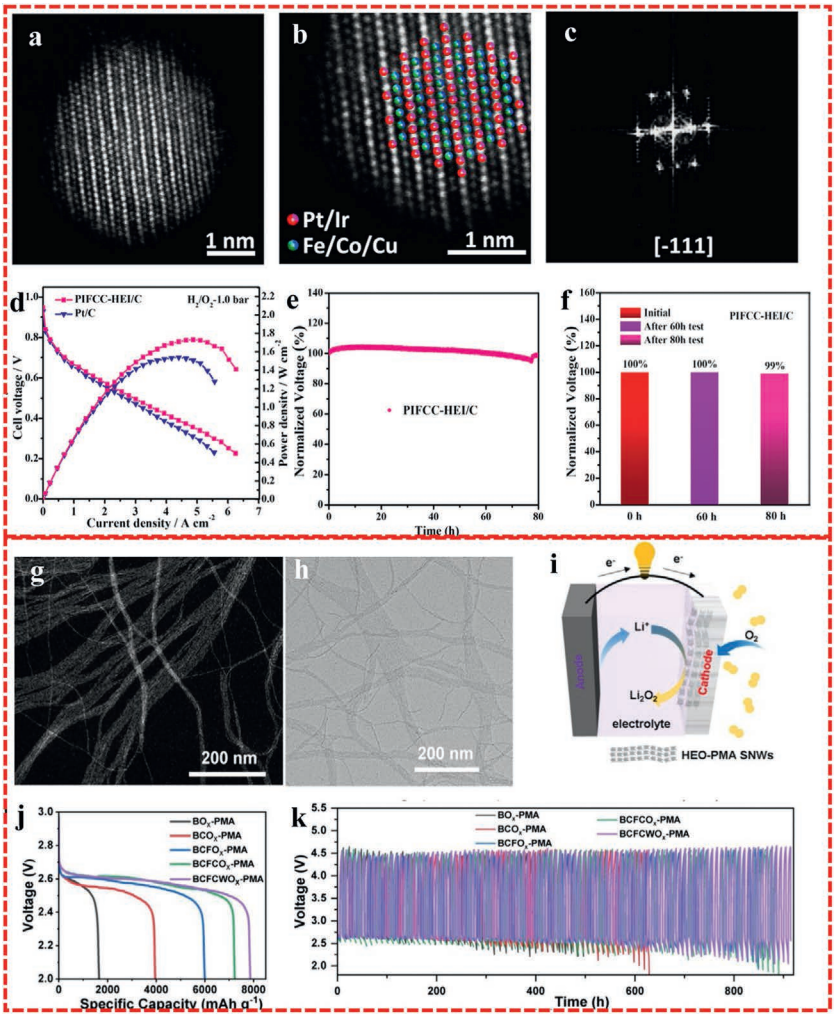


Fig. 4. Atomic structure and electronic structure characterization of PIFCC–HEIs. Atomically resolved HAADF-STEM image (a) and its enlarged image (b) of a PIFCC–HEI NP from the [1̄11] zone axis. (c) Corresponding fast Fourier transformation (FFT) pattern. (d) Polarization and power density curves of the H_2/O_2 fuel cell with PIFCC–HEI/C and commercial Pt/C as the cathode (0.10 mg $_{noble\ metal}$/cm^2) under O_2 pressure of 1.0 bar. (e) Long-term stability of the H_2/O_2 fuel cell with PIFCC–HEI/C as the cathode at a current density of 1 A/cm^2. (f) Quantitative comparisons of the stability shown in panel (e) at different times. Reproduced with permission [63]. Copyright 2023, ACS. (g) HAADF-STEM images of BCFCWPOx-PMA SNWs. (h) TEM image of BCFCWPOx-PMA SNWs. (i) Schematic illustration of the rechargeable HEO-PMA SNWs based LOB. (j) Deep discharge curves at a current density of 100 mA/g. (k) Cycling stability at 100 mA/g with a limited capacity of 500 mAh/g. Reproduced with permission [64]. Copyright 2025, ACS.

alkaline HOR [66]. They revealed that the strong interactions between different metal sites in HEA SNWs could greatly regulate the binding strength of protons and hydroxyl groups, thereby enhancing HOR activity. Various alcohols can be oxidized through the mechanism of alcohol molecule adsorption and further oxidation of CO. However, the slow kinetics of traditional monometallic or alloy catalysts severely limit the further application of electrocatalytic alcohol oxidation. The high-entropy effect exhibited by HEAs can integrate the advantages of multiple sites, and the synergistic mechanism can further accelerate reaction kinetics. The introduction of more non-precious metal elements in HEAs has also been reported. Zhang *et al.* [67] developed a wet-chemical hydrothermal method to synthesize PtCuNiCoFe HEA nanoparticles with enhanced compositional uniformity and precise performance control at ~170 °C for electrochemical methanol oxidation reaction (MOR). In addition to the tunability of elemental composition, the size effect on electronic state regulation should not be overlooked.

Li *et al.* [68] synthesized uniform and ultrasmall (~3.4 nm) $Pt_{18}Ni_{26}Fe_{15}Co_{14}Cu_{27}$ HEA *via* a simple low-temperature oil-phase strategy (Fig. 5a), which exhibited excellent bifunctional electrocatalytic performance for MOR (Figs. 5d and e). The suitable electronic environment of HEAs enabled multiple active sites for the appropriate adsorption of key intermediates and efficient electron transfer in the electrocatalytic process, thereby maximizing the utilization of surface electroactivity. To achieve higher atomic utilization, Jing *et al.* synthesized high-entropy catalysts with small sizes (~2.5 nm) and high-density dispersion (up to 80 wt%) *via in-situ* reduction of hydrogen boronene (Figs. 5b and c). Notably, due to the stable intermetallic compounds and strong metal-support interactions, annealing at 1000 °C did not cause sintering of these nanoparticles. They also exhibited excellent activity and stability in electrochemical reduction reactions. According to DFT calculations, the source of the significant electroactivity and durability of HEA in HER and MOR was attributed to the synergistic effect of each element on efficient electron transfer (Figs. 5f and g). From the above discussion, it can be inferred that HEMs with smaller sizes have significant research potential for reactions such as small-molecule catalysis [69].

5.2. Sub-nanometer HEMs in biomedical applications

The aforementioned studies indicate that HEMs possess significant potential for applications in the areas of water splitting, fuel cells, and small molecule oxidation. Compared to traditional cat-

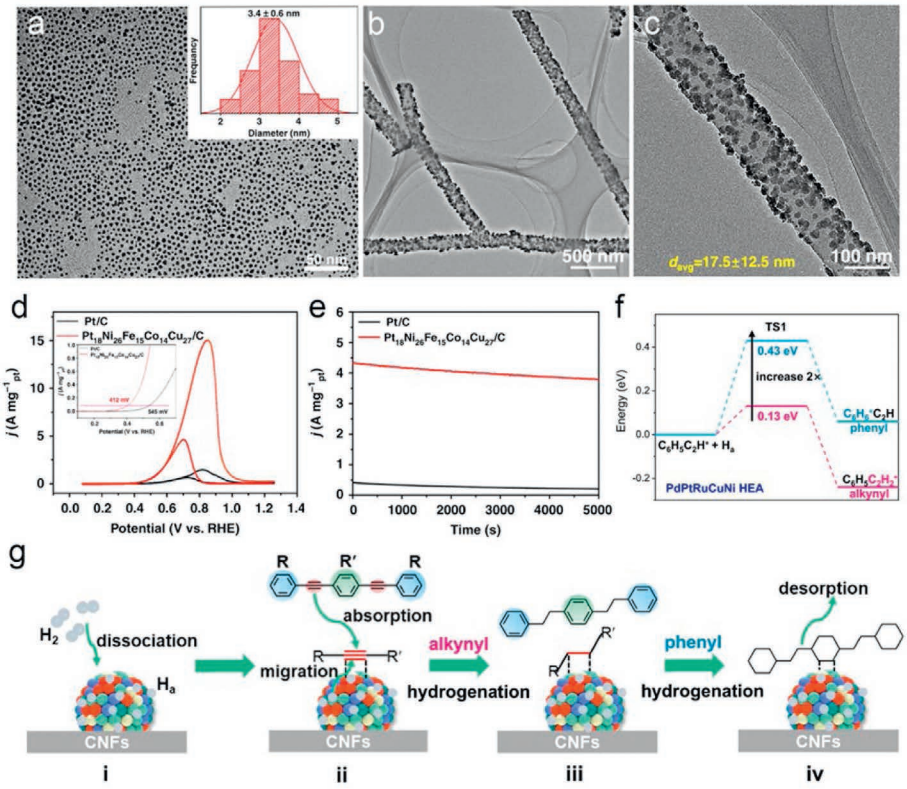


Fig. 5. (a) TEM images of $Pt_{18}Ni_{26}Fe_{15}Co_{14}Cu_{27}$ nanoparticles. (b) The morphologies. (c) HRTEM images of PdPtRuCuNi/CNFs. (d) CV curves (the inset is the onset potential, the mass activity of 0.1 A/mg) of Pt/C and $Pt_{18}Ni_{26}Fe_{15}Co_{14}Cu_{27}$/C. (e) Chronoamperometric tests for MOR at 0.65 V *vs.* RHE. (f) The first-step hydrogenation reaction barriers of the phenyl groups in phenylethane over PdPtRuCuNi (111), Pd (111), and Ru (111). (g) Reaction pathways for the hydrogenation of DEB over PdPtRuCuNi HEA nanocatalysts. Reproduced with permission [69]. Copyright 2020, Springer.

alysts, HEMs exhibit distinct advantages due to their high configurational entropy and sluggish diffusion and other effects. These advantages include low overpotentials, exceptional thermal stability, and rapid kinetics. As a result, HEMs hold great promise in the biomedical field, particularly in disease treatment, where they represent one of the most promising directions for the development of nanozymes [70–72].

Moreover, the advancement of multifunctional nanozyme systems that integrate targeting, imaging, and combinatorial therapies could further enhance the translational potential of these materials, offering substantial clinical value. In the realm of nanozymes, there have already been several studies focused on high-entropy-material nanozymes (HEMzymes). The construction of atomic-scale HEMzymes is of paramount importance for developing efficient catalytic systems and warrants further exploration. However, the inherent multielemental composition and small size of atomic-scale HEMzymes introduce significant thermodynamic instability. This presents a considerable challenge for the development of sub-nanometer high-entropy nanozymes (sn HEMzymes) [73–75]. Addressing this challenge will be crucial for harnessing the unique properties of HEMs and translating them into effective therapeutic applications. The exploration of HEMzymes not only advances our understanding of catalysis at the nanoscale but also opens new avenues for innovative biomedical applications. By leveraging the unique characteristics of HEMs, researchers can potentially develop novel therapeutic strategies that are more effective and tailored to specific medical needs, ultimately contributing to improved patient outcomes.

5.2.1. Biological nanoenzymes

Nanozymes are clearly defined as artificial enzyme mimetics based on nanomaterials. Due to their exceptional environmental tolerance, recyclability, and long-term stability, they are gradually emerging as viable alternatives to natural enzymes [76–78]. In Figs. 6a and b, Zhang *et al.* reported a MnFeCoNiCu transition metal HEMzymes that leverages the unique surface atomic configuration and pronounced d-orbital coupling characteristics of its multimetallic components. DFT calculations indicated that the d-orbital coupling among different metals increases the electron density near the Fermi level (EF) and induces a shift in the center of the entire d-band. This enhancement improves the efficiency of electron transfer while also boosting peroxidase (POD)-like activity, making it promising for biosensing and antimicrobial applications [79]. He and his collaborators designed a Ru-based HEMzymes (RuPtIrRhCu) with simultaneously enhanced catalytic activity and stability. It was demonstrated that the preferred adsorption site for the nanozyme is the Ru atom, which exhibits a "hydroxyl spillover" effect from Ru to Pt, resulting in a more favorable catalytic pathway with lower energy barriers compared to single-metal sites (Cu, Ir, Rh, and Ru) in Fig. 6c. Consequently, this nanozyme exhibits notable POD-like activity and stability. Additionally, a multichannel sensing platform was developed based on this system to screen various biological antioxidants and achieve precise discrimination of chiral cysteine (Cys) [80]. In addition, Li *et al.* utilized DFT calculations and the Sabatier principle to demonstrate that self-polymerized polydopamine (PDA) surface engineering moderately lowers the d-band center of HEAs, optimizes the surface charge distribution, and enhances the adsorption-desorption efficiency of substrates. For better application, the study innovatively integrated HEzymes@PDA with hydrogels for biosensing analysis. This research highlights the significant potential of high-entropy alloys in catalytic sensing applications [81].

5.2.3. Anti-tumor treatment

In addition to the mechanism of removing reactive oxygen species (ROS), HEMs can also generate ROS through the endoge-

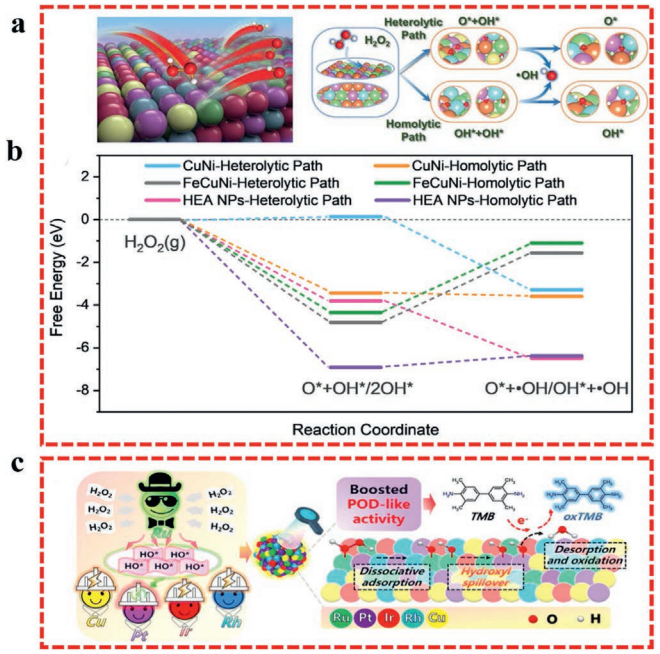


Fig. 6. (a) Scheme showing the surface reactivity of the HEA NPs during POD, like activity and different reaction pathways for the decomposition of H_2O_2 to generate •OH on the HEA NPs with optimization. (b) Optimized free energy profiles for H_2O_2 decomposition along different pathways on the CuNi, FeCuNi, and HEA NPs. Reproduced with permission [79]. Copyright 2023, Wiley-VCH. (c) Schematic diagram for hydroxyl spillover mechanism in POD-like catalysis of RuPtIrRhCu HEAzymes. Reproduced with permission [80]. Copyright 2025, RSC.

nous environment for disease treatment, showing significant potential for application, particularly in tumor therapy [82,83].

Pavithra *et al*. explores one-dimensional Fe-Co-Ni-Cu-Zn HEA nanowires (NWs) as biocompatible nanostructures with therapeutic potential, demonstrating approximately 80 % cell viability and effective photothermal therapy (PTT) against murine melanoma cells. This research highlights the potential of HEA NWs as innovative materials for cancer therapy in Fig. 7a [84]. Recent research has further expanded the applications of high-entropy alloy nanoparticles (HEANPs) by developing ultra-small high-entropy alloy nanoparticles (US-HEANPs), providing a new solution for tumor therapy. In Fig. 7b, these PtPdRuRhIr US-HEANPs possess strong photothermal conversion capabilities, converting near-infrared light into thermal energy and successfully eliminating cancer cells [85].

The physicochemical advantages of HEMs are also reflected in their ability to reprogram the tumor microenvironment (TME) and provide anti-tumor treatment through cascade nanozyme-activated chemical dynamics and immune synergistic therapy. For example, Wang *et al*. demonstrated a multifunctional high-entropy two-dimensional layered double hydroxide (HE-LDH) nanoplatform that reprograms the tumor microenvironment through synergistic cascade reactions, not only triggering a ROS storm and depleting glutathione/GPX4 but also stimulating the activation of the cGAS/STING pathway, thereby achieving the effect of inhibiting tumor growth in Fig. 6c [75]. This study expands the possibilities for applying HEMs in the medical field in Fig. 7c [86].

5.2.2. Antibacterial and anti-inflammatory

Furthermore, HEMs not only possess significant advantages in terms of antibacterial and anti-inflammatory properties but also play a role in wound healing and the treatment of biofilm formation, presenting a promising future in biomedical applications.

He *et al*. explored the application of high-entropy MXenes (HE MXenes) in the field of antibacterial, particularly their effectiveness against methicillin-resistant *Staphylococcus aureus* (MRSA) in Fig. 8a. By introducing multiple transition metal elements, the researchers successfully prepared HE MXenes with excellent photothermal conversion efficiency and enzyme-mimicking activity. And thereby assisting in the treatment of bacterial keratitis and subcutaneous abscesses caused by MRSA [87]. Similarly, a functional heterojunction composed of Ti_3C_2-MXene and $(CoCrFeMnNi)_3O_4$ HEO has been developed, achieving synergistic photodynamic and mild photothermal therapy for treating skin biofilm infections through the valence electron fluctuation effect. Under near-infrared light irradiation, photogenerated hot electrons from MXene are efficiently transferred to the HEO surface, significantly enhancing ROS generation. At the same time, the built-in electric field suppresses electron-hole recombination, ensuring the efficient photothermal-photodynamic synergy and reducing excessive heat generation (Fig. 8b) [88]. In addition to the composite with carriers, studies have also reported on the antibacterial and antibiofilm properties of HEA-NPs under photothermal assistance. Research shows that HEA-NPs can rapidly heat up under sunlight,

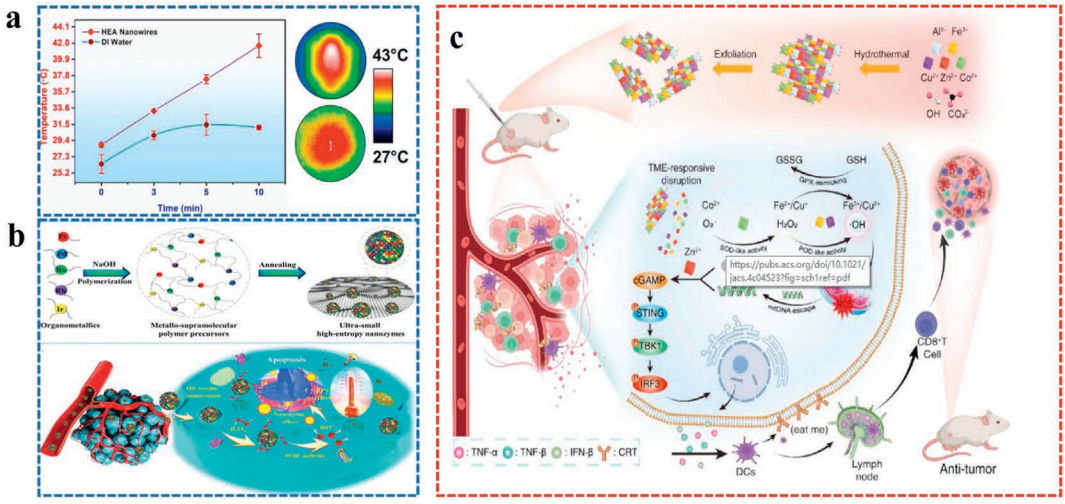


Fig. 7. (a) Photothermal efficacy of one-dimensional Fe-Co-Ni-Cu-Zn HEA NWs [84]. (b) Fabrication of PtPdRuRhIr US-HEANPs by metal-ligand cross-linking strategy and for enhancing tumor photothermal therapy. Reproduced with permission [85]. Copyright 2023, Wiley-VCH. (c) Schematic diagram of the synthetic process of HE-LDH and its anti-tumor strategy of NCDT and immune synergistic therapy. Reproduced with permission [86]. Copyright 2021, Wiley-VCH.

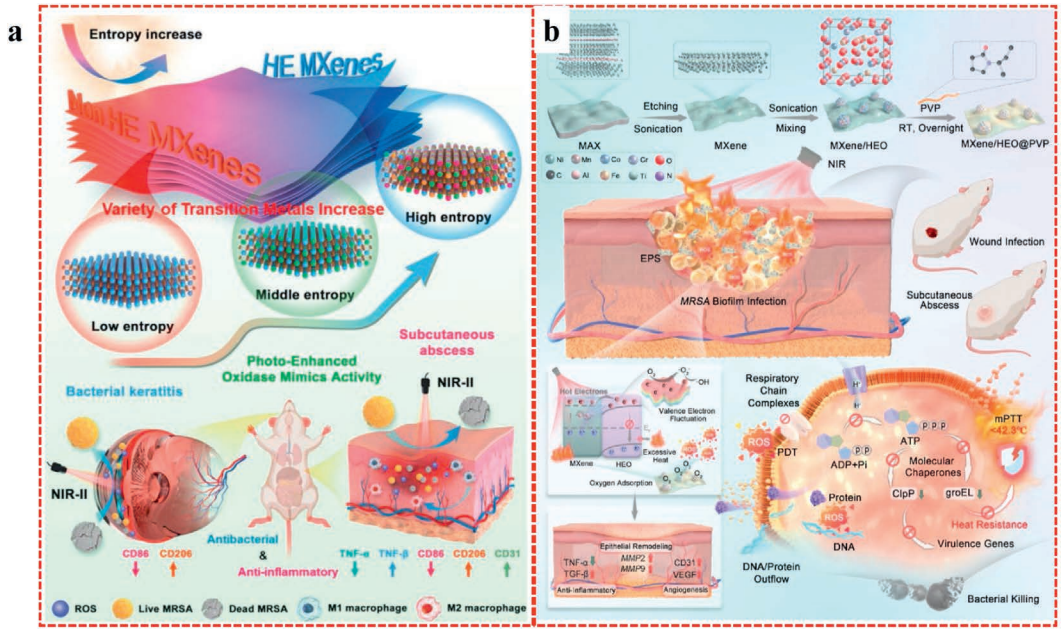


Fig. 8. (a) Schematic illustration of engineering monolayer high-entropy MXenes (HE MXenes) nanotherapeutic for treating bacterial keratitis and subcutaneous abscess induced by MRSA. Reproduced with permission [87]. Copyright 2023, Wiley-VCH. (b) Schematic of the HEO achieving photodynamic therapy (PDT)/mild-PTT (mPTT) multimodal antibacterial effects in MRSA wound infection and subcutaneous abscess. Reproduced with permission [88]. Copyright 2023, Wiley-VC.

generating high temperatures that destroy bacterial cells and remove biofilms. Through the synergistic effect of copper ion release and thermal damage, more ROS are generated, significantly improving antibiofilm efficiency, reaching 97.4%. This study provides a new solution for biofouling and microbial corrosion caused by marine microorganisms [89].

6. Summary and outlook

We have briefly summarized the advantages of sub-nanometer HEMs and their research progress in electrocatalysis and biomedicine. Reported studies have demonstrated that small-sized, especially sub-nanometer-sized, HEMs exhibit excellent activity and stability. Their multifunctional characteristics endow them with significant potential in energy storage and conversion as well as in medical diagnostics and treatment [90–93]. The following discusses the existing challenges and future research directions.

(1) Synthesis: There is a need for safer, more efficient methods to produce sub-nanometer HEMs. Current techniques often require harsh conditions and focus on limited precious metal components. Improving synthesis methods and expanding element selection is essential for better control over composition and morphology, enabling broader applications.
(2) Material characterization: The unique multi-component and small-sized nature of sub-nanometer HEMs relies on high-resolution techniques like HAADF-STEM, XAFS, and XPS. Given their high surface reactivity, developing refined characterization techniques, such as atomic-level methods, is crucial to capture dynamic changes in these materials.
(3) Synthesis and reaction mechanisms: The reactivity of sub-nanometer HEMs is often linked to existing catalytic mechanisms, but the presence of multiple active sites and unique quantum effects should also be considered. Researchers should adopt a “trial and error” approach in synthesis and performance exploration, focusing on systematic high-throughput calculations and new catalytic mechanisms.
(4) Applications: Sub-nanometer HEMs have potential in catalysis, improving reaction rates in the field of energy catalysis. Enhance energy storage in batteries and supercapacitors, and can be tailored for sensitive sensors, magnetic storage, and environmental remediation, showcasing their multifunctionality. In biomedical applications, bioimaging and drug delivery are very promising research directions. However, they also face several challenges, including those related to biocompatibility, manufacturing complexity, stability, functionalization difficulties, regulatory issues, and unclear biological distribution and clearance mechanisms.

Declaration of competing interest

The authors declare that they have no known competing financial interests or personal relationships that could have appeared to influence the work reported in this paper.

CRediT authorship contribution statement

Zhiyu Shao: Writing – original draft. **Shaohua Wang:** Writing – original draft. **Haijia Yu:** Writing – review & editing. **Diyang Shan:** Writing – review & editing. **Zhiyu Tang:** Writing – review & editing. **Yihang Fu:** Writing – review & editing. **Jianshi Du:** Writing – review & editing, Visualization. **Jianhua Liu:** Writing – review & editing, Visualization. **Keke Huang:** Writing – review & editing, Visualization, Supervision.

Acknowledgments

This work was supported by the Jilin Provincial Natural Science Foundation (No. YDZJ202501ZYTS291) and the Changchun National Key Laboratory Major Project (No. 2024GZZ02).

References

[1] S. Schweidler, M. Botros, F. Strauss, et al., Nat. Rev. Mater. 9 (2024) 266–281.
[2] C.H. Cui, S.H. Yu, Acc. Chem. Res. 46 (2013) 1427–1437.
[3] R.N. Guo, Y. Yang, C.C. Zhao, et al., Adv. Funct. Mater. 34 (2024) 2313168.
[4] Y.Y. Zhai, X.R. Ren, B.L. Wang, S.Z. Liu, Adv. Funct. Mater. 32 (2022) 2207536.

[5] L.L. Han, S.Y. Zhu, Z.Y. Rao, et al., Nat. Rev. Mater. 9 (2024) 846–865.
[6] M.C. Mackey, Rev. Mod. Phys. 61 (1989) 981.
[7] L.M. Martyushev, V.D. Seleznev, Phys. Rep. 426 (2006) 1–45.
[8] Y.J. Ma, Han Du, S. Zheng, et al., Energy Storage Mater. 79 (2025) 104295.
[9] S.R. Li, J.L. Gong, Chem. Soc. Rev. 43 (2014) 7245–7256.
[10] H. Heinz, H. Ramezani-Dakhel, Chem. Soc. Rev. 45 (2016) 412–448.
[11] H. Gleiter, Acta Mater. 56 (2008) 5875–5893.
[12] E. Davoodi, H. Montazerian, A.S. Mirhakimi, et al., Bioact. Mater. 15 (2022) 214–249.
[13] Q. Dong, Y. Zhang, Y. Chen, Intermetallics 187 (2025) 109001.
[14] W.L. Hsu, C.W. Tsai, A.C. Yeh, J.W. Yeh, Nat. Rev. Chem. 8 (2024) 471–485.
[15] Y.K. Hua, G.J. Su, Q.Q. Li, et al., Crit. Rev. Env. Sci. Tec. 55 (2025) 25–48.
[16] L.L. Yang, R. He, J.L. Chai, et al., Adv. Mater. 37 (2025) 2412337.
[17] A.T. Fenley, H.S. Muddana, M.K. Gilson, Proc. Natl. Acad. Sci. U. S. A. 109 (2012) 20006–20011.
[18] A.A. Khan, S. Razzaq, A. Khan, F.K. Owais, Renew. Sust. Energ. Rev. 42 (2015) 773–785.
[19] Y.F. Sun, S. Dai, Sci. Adv. 7 (2021) eabg1600.
[20] W. Yang, S. Pang, Y. Liu, Intermetallics 141 (2022) 107421.
[21] J.S. Chae, S.K. Park, K.C. Roh, H.S. Park, Energy Storage Mater. 24 (2020) 113–128.
[22] Z.J. Shi, Q.H. Fang, P.K. Liaw, J. Li, Adv. Eng. Mater. 25 (2023) 2300968.
[23] P.C. Chen, M.Y. Gao, C.A. McCandler, et al., Nat. Nanotechnol. 19 (2024) 775–781.
[24] C.Z. Ning, L.T. Dou, P.D. Yang, Nat. Rev. Mater. 2 (2017) 17070.
[25] J.M. Zhang, H.B. Yang, D.J. Zhou, B. Liu, Chem. Rev. 122 (2022) 17028–17072.
[26] S.J. Lombardo, A.T. Bell, Surf. Sci. Rep. 13 (1991) 3–72.
[27] H. Wang, J.M. Chen, Y.P. Lin, et al., Adv. Mater. 33 (2021) 2008422.
[28] W.J. Xu, Y.C. Bai, Y.D. Yin, Adv. Mater. 30 (2018) 1802091.
[29] V. Artero, Nat. Energy 2 (2017) 17131.
[30] C. Deng, T. Wang, P. Wu, W. Zhu, S. Dai, Nano Energ. 120 (2024) 109153.
[31] M.G. Li, F.X. Lin, S.P. Zhang, et al., Sci. Adv. 10 (2024) eadn2877.
[32] E. Roduner, Chem. Soc. Rev. 35 (2006) 583–592.
[33] X.Y. Yan, Y.S. Zhou, S.Y. Wang, Adv. Funct. Mater. 35 (2025) 2413115.
[34] X.Y. Wang, Q.D. Liu, X. Wang, Adv. Funct. Mater. 35 (2025) 2504275.
[35] S. Chen, Y.H. Wang, G. Pu, et al., Energy Fuels 37 (2022) 36–57.
[36] L. Chang, H.C. Jing, C. Liu, C.T. Qiu, X. Ling, Adv. Sci. 11 (2024) 2406521.
[37] Z.S. Meng, Z.J. Xu, H.W. Tian, W.T. Zheng, Materi. Horiz. 10 (2023) 3293–3303.
[38] B. Ni, Y.A. Shi, X. Wang, Adv. Mater. 30 (2018) 1802031.
[39] N. Rasooli, W. Chen, M. Daly, Nanoscale 16 (2024) 1650–1663.
[40] B. Wang, Y.F. Yao, X.W. Yu, et al., J. Mater. Chem. A 9 (2021) 19410–19438.
[41] K. Li, W. Chen, Mater. Today Energy 20 (2021) 100638.
[42] H.X. Li, X.L. Sun, H.T. Huang, Prog. Mater. Sci. 148 (2025) 101382.
[43] Z.Y. Wang, J.H. You, Y. Zhao, et al., J. Environ. Chem. Eng. 11 (2023) 109080.
[44] R. Nartita, D. Ionita, I. Demetrescu, Cryst. 14 (2024) 451.
[45] Y.F. Ye, Q. Wang, J. Lu, C.T. Liu, Y. Yang, Mater. Today 19 (2016) 349–362.
[46] Y.G. Yao, Q. Dong, A. Brozen, et al., Science 376 (2022) eabn3103.
[47] P. Jain, P. Hosseini, A. Kostka, et al., Faraday Discuss. 264 (2026) 207–230.
[48] H.Y. Qiao, M.T. Saray, X.Z. Wang, et al., ACS. Nano 15 (2021) 14928–14937.
[49] J.F. Luan, K. Ma, L.Y. Zhang, et al., Curr. Org. Chem. 14 (2010) 683–698.
[50] H. Thürlová, F. Průša, Materials 15 (2022) 7899.
[51] H.F. Que, B.X. Li, L.H. Sun, et al., Nat. Synth. 4 (2025) 582–591.
[52] Y.G. Yao, Z.N. Huang, P.F. Xie, et al., Science (1979) 359 (2018) 1489.
[53] P. Ball, L. Garwin, Nature 355 (1992) 761–764.
[54] H. Schmidt, F. Giustiniano, G. Eda, Chem. Soc. Rev. 44 (2015) 7715–7736.
[55] Q.D. Liu, X. Wang, Chem. Catal 2 (2022) 1257.
[56] Z.S. Li, B.L. Li, M. Yu, C.L. Yu, Int. J. Hydrogen. Energy 47 (2022) 26956.
[57] S. Zhang, T. Hedtke, X. Zhou, M. ElimelechJae, H. Kim, ACS ES&T Eng. 1 (2021) 706.
[58] T. Zhang, H.F. Zhao, Z.J. Chen, et al., Nat. Commun. 16 (2025) 3327.
[59] M.J. Cui, C.P. Yang, B.Y. Li, et al., Adv. Energy Mater. 11 (2021) 2002887.
[60] H.Z. Cai, S.Z. He, H.P. Yang, et al., Adv. Mater. 37 (2025) 2508610.
[61] H.Y. Qiao, X.Z. Wang, Q. Dong, et al., Nano Energy 86 (2021) 106029.
[62] L.P. Yao, F.R. Zhang, S. Yang, et al., Adv. Mater. 36 (2024) 2314049.
[63] G. Feng, F.H. Ning, Y. Pan, et al., J. Am. Chem. Soc. 145 (2023) 11140–11150.
[64] H.Y. Ge, W.X. Shi, J.L. Liu, Y. Zhang, X. Wang, J. Am. Chem. Soc. 147 (2025) 8367–8376.
[65] Y.M. Hu, T.T. Chao, Y.H. Dou, et al., Adv. Mater. 37 (2025) 2418504.
[66] C.H. Zhan, Y. Xu, L.Z. Bu, et al., Nat. Commun. 12 (2021) 6261.
[67] Z.X. Zhang, P.P. Yu, Z.J. Liu, et al., J. Am. Chem. Soc. 147 (2025) 9640–9652.
[68] H.D. Li, Y. Han, H. Zhao, et al., Nat. Commun. 11 (2020) 5437.
[69] Z.K. Jing, Y.K. Guo, Q. Wang, et al., Nat. Commun. 15 (2024) 5806.
[70] Y. Yuan, L. Chen, K.X. Song, et al., Nat. Commun. 15 (2024) 5636.
[71] L. Ma, J.J. Zheng, N. Zhou, et al., Nat. Commun. 15 (2024) 233.
[72] C. Liu, L. Gui, J.J. Zheng, et al., J. Am. Chem. Soc. 145 (2023) 19086.
[73] N. Kar, M. McCoy, J. Wolfe, et al., Nat. Synth. 3 (2024) 175.
[74] C. Wang, F.Y. Yuan, Z.C. Yan, et al., J. Am. Chem. Soc. 147 (2025) 136.
[75] C.J. Ding, J. Min, Y.K. Tan, et al., Adv. Mater. 36 (2024) 2401361.
[76] H. Wei, E. Wang, Chem. Soc. Rev. 42 (2013) 6060.
[77] Y.Y. Huang, J.S. Ren, X.G. Qu, Chem. Rev. 119 (2019) 4357.
[78] L.J. Huang, D.W. Sun, H.B. Pu, et al., Compr. Rev. Food Sci. Food Saf. 18 (2019) 1496.
[79] J.X. Feng, X.W. Yang, T. Du, et al., Adv. Sci. 10 (2023) 2303078.
[80] Q. Yang, J.W. Zhang, Y.X. Tang, et al., Chem. Sci. 16 (2025) 10842–10851.
[81] K.Y. Feng, H.T. Wang, S. Zhou, et al., Adv. Sci. 12 (2025) 2502354.
[82] R.X. Zhao, Y.L. Zhu, L.L. Feng, et al., Adv. Mater. 36 (2024) 2307115.
[83] C.H. Li, H.W. Cheng, Z.Q. Zhuang, et al., Small Methods 9 (2025) 2500231.
[84] C.L.P. Pavithra, S.A. Sankaranarayanan, M. Pebam, et al., Mater. Lett. 312 (2022) 131659.
[85] Y.J. Ai, M.Q. He, H. Sun, et al., Adv. Mater. 35 (2023) 2302335.
[86] P.P. Liang, B. Ballou, X.Y. Lv, et al., Adv. Mater. 33 (2021) 2005155.
[87] X. He, Y. Qian, C. Wu, et al., Adv. Mater. 35 (2023) 2211432.
[88] Y.X. Li, L.L. Yang, Y.J. Liao, et al., Adv. Funct. Mater. 33 (2023) 2302712.
[89] R. Zhang, W.W. Li, Z.C. Guo, et al., ACS Nano 19 (2025) 21348–21364.
[90] J. Sun, W. Liu, F. Liang, et al., Adv. Funct. Mater. 36 (2026) e10855.
[91] N. Kar, S.E. Skrabalak, Nat. Rev. Mater. 10 (2025) 638–653.
[92] W.L. Hsu, C.W. Tsai, A.C. Yeh, J.W. Yeh, Nat. Rev. Chem. 8 (2024) 471–485.
[93] C.Y. Li, Z.C. Zhang, K.L. Zhu, et al., Nat. Synth. 4 (2025) 1422–1434.